

GROUND OPTICAL NAVIGATION FOR THE STARDUST-NEXT MISSION TO COMET 9P/TEMPEL 1

**Stephen D. Gillam, J. Ed. Riedel, William M. Owen Jr.,
Tseng-Chan Mike Wang, Robert A. Werner, Shyam Bhaskaran,
Steven R. Chesley, Paul F. Thompson, and Aron A. Wolf***

Ground-based optical navigation (OpNav) using pictures taken by the Navigation camera on the Stardust spacecraft provided the target-relative information needed to design maneuvers during its approach to comet Tempel 1. Hardware problems, limited downlink bandwidth, and changes in the flight profile affected the OpNav picture schedule, sometimes in near-real time. The Stardust navigation camera and attitude control presented challenges. Picture-processing techniques were developed during approach that included background estimation, co-addition, and co-registration. These techniques, along with adaptive picture scheduling, successfully addressed the challenges.

INTRODUCTION

Stardust-NExT (New Exploration of Tempel 1) is the extension of the Stardust Mission which studied the asteroid (5535) Annefrank¹ and collected samples from the coma of comet 81P/Wild 2. The prime mission was completed January 15, 2006, when the sample return capsule returned to Earth. Operating for more than 12 years, the Stardust spacecraft encountered comet 9P/Tempel 1 on February 15, 2011, previously visited by the Deep Impact spacecraft on July 4, 2005. Stardust is the first mission to return a sample of cometary dust to Earth. Stardust-NExT is the first mission to acquire images of a previously visited comet. The objectives of the Stardust-NExT imaging science are to extend the current understanding of the processes that affect the surfaces of comet nuclei by documenting the changes that have occurred on comet Tempel 1 between two successive perihelion passages, extend the geologic mapping of the nucleus of Tempel 1 to elucidate the extent and nature of layering, help refine models of the formation and structure of comet nuclei, and extend the study of smooth flow deposits, active areas, and known exposure of water ice². A secondary objective was to characterize the crater produced by the Deep Impact impactor spacecraft³ 4 July 4 2005, to better understand the structure and mechanical properties of cometary nuclei and elucidate crater formation processes on them. At minimum, the mission was to return at least one stereo image pair at a resolution of 20 m/pixel or better with a stereo separation angle between 10 and 30°, and to image at least 25% of the hemisphere seen by deep Impact at 80 m / pixel or better with the Stardust navigation camera (NavCam)⁴. These requirements drove the

* All authors are at the Jet Propulsion Laboratory, California Institute of Technology, MS 301-121, 4800 Oak Grove Drive, Pasadena. CA 91109.

navigation effort. In this paper we shall use the terms “OpNav” and “opnav” to mean optical navigation and optical navigation pictures respectively.

OpNav is the application of narrow-field astrometry to spacecraft orbit determination. Opnavs of a target body – in the case of Stardust-NEXT comet 9P/Tempel 1– against a background of reference stars provide a measurement of the apparent right ascension and declination of the target as seen from the spacecraft. These angular observations provide the only direct information about the spacecraft-to-comet vector.⁵ The spacecraft’s heliocentric trajectory is already well determined from radiometric orbit determination (OD); the comet’s *a priori* ephemeris is determined from Earth-based astrometry. Opnavs thus provide the third leg of the Sun-spacecraft-comet triangle. The close flyby required kilometer-level accuracy that could only be provided by opnavs of the comet. From 30 minutes before the encounter the OpNav took place onboard with an autonomous navigation system (AutoNav)⁶; until then it happened on the ground. This paper concentrates on the ground OpNav.

The Stardust-NEXT OpNav was challenging in several ways. The largest technical challenge was to provide accurate measurements of the comet pixel position in the NavCam in the presence of a large and variable background, a fixed pattern of hot pixels, and with smeared images of the stars and comet. The main logistical challenge was to process more than three hundred pictures in the three days just prior to the autonomous navigation system (Autonav) taking over the OpNav.

The final opnavs from Encounter(E)-80 hours to E-42 hours were crucial to successfully targeting the spacecraft to the comet. They allowed the navigation team to determine if they were seeing the nucleus through the coma or the periodic motion of the comet’s center of brightness as the somewhat elongated nucleus rotated about its center of mass. The final set of ground-based opnavs at E-42 hours and the latest comet ephemeris from JPL’s Solar System Dynamics (SSD) group, that did not include those opnavs, were used by the OD team to provide the comet ephemeris for the Autonav filter.

This paper will discuss these and other challenges, review the performance of the ground OpNav, discuss the NavCam and the attitude control system as they affected the OpNav effort, the planning and in-flight modification of the opnav picture schedule, how the mission design affected OpNav processing, how OpNav fitted into the flight operations, the evolution of comet position measurements during the approach to Tempel 1, OpNav team staffing, and the lessons learned from the mission.

THE FLIGHT SYSTEM

The flight system, as it affected navigation, is shown in Figure 1. It includes two solar panels, a high-gain antenna (HGA), a medium-gain antenna (MGA), four clusters of two 4.45 N trajectory control maneuver (TCM) thrusters and two 0.89 N reaction control system (RCS) thrusters, two Whipple shields, a periscope, and a stationary navigation camera (NavCam) with a scanning mirror. The thrusters are located on the bottom corners of the spacecraft bus and point in the $-Z$ direction. The TCM thrusters were used for maneuvers and the RCS thrusters were used for attitude changes. The scanning mirror is set at 45° to the NavCam optic axis (pointing in the $-Y$ direction) and rotates about it to rotate the NavCam field of view from the $+X$ direction (forward), through the $-Z$ direction to the $-X$ direction (aft). The forward view (at 0°) is through the periscope which protects the scan mirror. The mirror’s rotates from -20° , at which the camera sees a black object on the spacecraft, to $+200^\circ$, allowing views up to 20° beyond the aft direction. Rolling the spacecraft to put the spacecraft-comet vector in the negative half of the $X-Z$ plane and rotating the mirror at the proper rate enables comet tracking during flybys. (The Autonav system commanded the

scanning mirror directly during flybys.) The maximum mirror rotational rate of the mirror is approximately 3.1 °/s.

Reaction wheels were not included for attitude control; this was achieved with the thrusters. The default spacecraft attitude was to point the HGA at the Earth for communications and radiometric orbit determination. For imaging, the spacecraft was pitched (rotated about the Y-axis) to place the comet below the plane of the solar panels because the scanning mirror could not see over them. A combination of pitches and mirror angles was used to put the comet or a calibration star in the NavCam field of view. The periscope is an optical assembly that allows the scanning mirror to look over the Whipple shield while it is pointed forward. This was to protect the scanning mirror from particle collisions that would significantly degrade its performance while flying through cometary comas.

The periscope contains two rectangular mirrors mounted at 45 degrees with respect to the spacecraft +X-axis. The mirrors are made out of aluminum to reduce the rate and amount of degradation from particle impacts. Post-Wild 2 encounter images through the periscope showed it to have been heavily damaged by the particle bombardment during encounter, as expected. For most of the Tempel 1 approach the spacecraft flew backwards toward the comet to avoid imaging through the periscope. At E-7 days, when it was necessary to fly forwards, spacecraft attitudes for imaging, requiring pitch maneuvers, were picked so that the scanning mirror angle could be large enough ($> 20^\circ$) to avoid looking through the periscope.

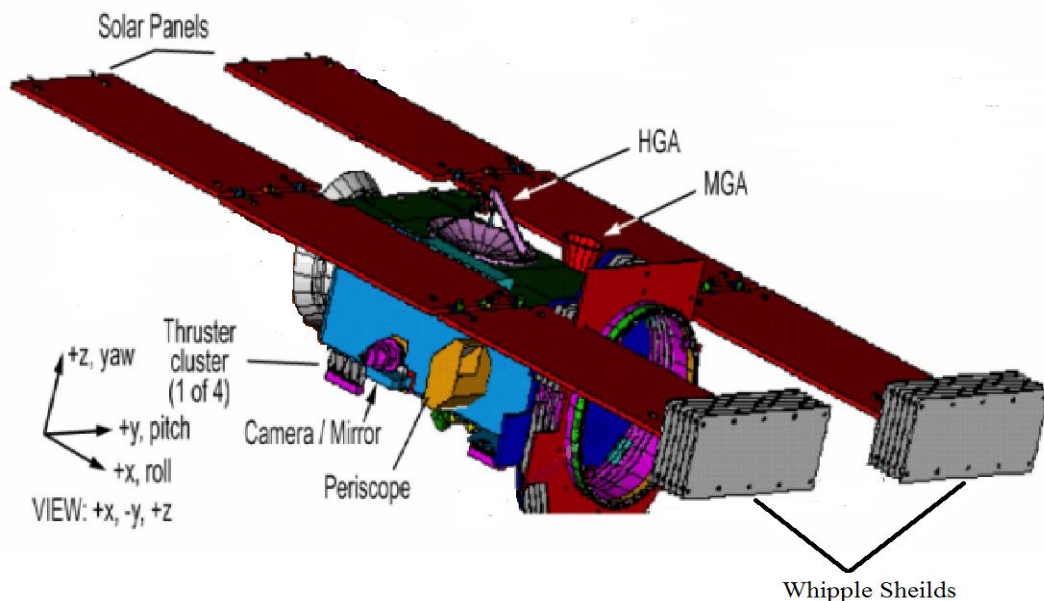


Figure 1. The Flight System⁴. The body-fixed, +Z direction is through the HGA, the +X direction is the direction of forward motion, which is through the Whipple dust shields, and the +Y direction completes a right-handed coordinate system.

The NavCam

The NavCam is used to optically navigate the spacecraft on approach to the comet to achieve the proper flyby distance.⁷ The NavCam consists of the following major functional elements: optics, filter wheel and shutter mechanisms, detector, scanning mirror, and control electronics. These are

shown in Figure 2. The optics and the filter-wheel and focal-plane shutter subassembly are inherited hardware designed, built, and tested for the Voyager Project. The NavCam has a scanning mirror mechanism, developed for Stardust, to vary the camera viewing angle.

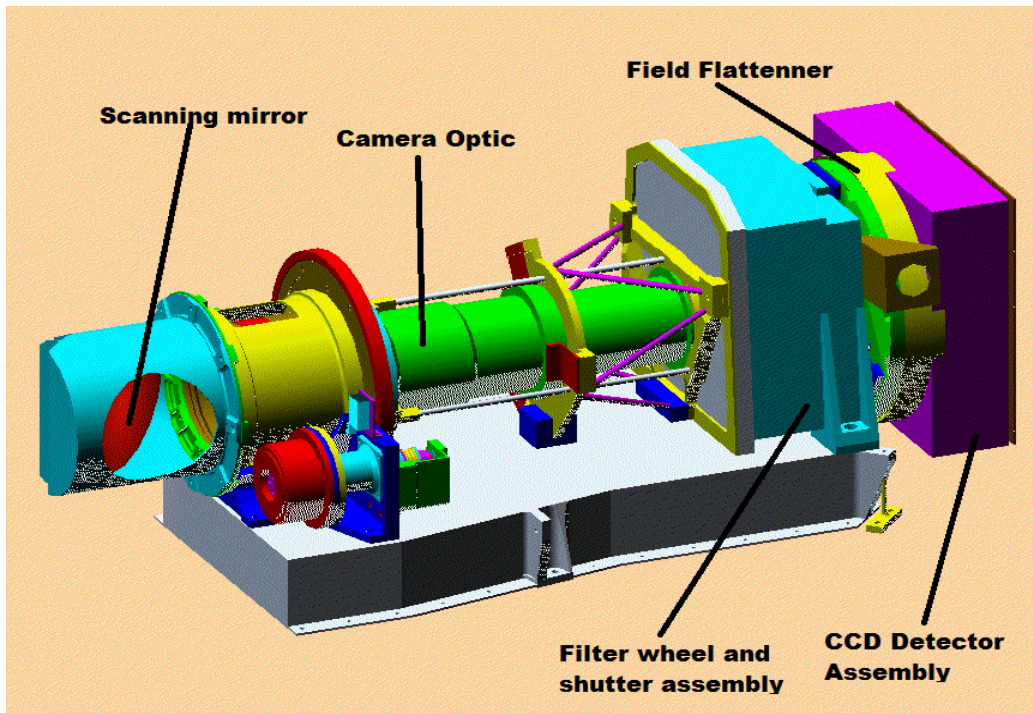


Figure 2. The Stardust NavCam⁸

The detector is a framing charge coupled device (CCD) imager developed for Cassini. The CCD is passively radiatively cooled to approximately -35C to suppress dark current, and to minimize proton, gamma and neutron radiation effects. The CCD is mounted in a hermetically sealed package which is back-filled with argon and shielded from protons and electrons. The CCD control and communication electronics are located in the sensor head behind the CCD. There are also options for 12 bit to 8 bit square root compression, windowing and error free compression within windows. OpNav pictures were taken with 12-bit resolution and no compression. The NavCam is also a science instrument. Its properties are listed in Table 1.

The optics is a six-element Petzval-type, refractor lens. A field flattener element, located in front of the CCD window, was designed for Stardust to reduce field curvature and to provide additional CCD radiation shielding. The optical barrel assembly mounts to the filter wheel. The filter wheel assembly contains an eight position filter wheel and a driving mechanism. Because radiation-resistant optical materials were used, the lens has a poor broad band modulation transfer function (MTF). The theoretical MTF for the spectral range 380 nm to 1100 nm is 30% at 32 lp/mm. The thickness of each filter is optimized to improve the MTF over that filter's passband.

The shutter assembly is a two-blade focal plane mechanism. A total of 4096 exposure durations are available from 5 ms to 20 s, in 5 ms increments. There is also a "bulb" command, for longer exposures, that allows the shutter to be held open for any length of time⁸. Bulb mode was also

used, prior to the filter wheel failure, in conjunction with a narrow-band filter to protect the Nav-Cam from accidental exposure to direct sunlight during a safing event. The shutter would be held open to prevent warping of the thin blades. Bulb mode was disabled during the NExT mission because the narrow band filters were not available.

Table 1. Nominal NavCam Properties.

Parameter	Units	Value
Aperture	cm	20
CCD format	pixels	1024x1024
Pixel size	μm	12 (square)
Charge capacity	electrons/pixel	100,000
Charge transfer efficiency	None	0.99996
Dark current	electrons/pixel/second	0.1
Read noise	electrons/pixel (RMS)	15
Focal length	Mm	200
Pixel scale	$\mu\text{rad/pixel}$	60
Field of view	degrees	3.5x3.5
Focal ratio	None	f/3.5
Digitization	Bits	12

Camera Bakes

A year after launch the filter wheel was found to be stuck at the OpNav filter, which transmits light from about 400 to 900 nm and has the greatest total throughput of any of the eight filters.⁹ The Petzval lens system suffers from some chromatic aberration over this large spectral range; resulting in an intrinsic point spread function of approximately 2.3 pixels. The camera optic was manufactured in the early 1970s and it is believed that its antireflection coatings have degraded. As a result, all images exhibit a broad shallow skirt of scattered light.

On a number of occasions contamination by a coating of unknown source and composition was found to exist inside the sealed optics. At times, it reduced the sensitivity of the camera to as much as a factor of 100 less than expected. Turning the spacecraft to place direct sunlight on the radiator, normally used to cool the detector, to raise the detector temperature to 24 C, for 30 minutes significantly reduced the contamination, presumably by evaporating it off the surfaces on which it had previously condensed. This procedure is known as a “camera bake.” The camera then showed sensitivity approaching that originally expected and significantly reduced scattered light.

Because of these experiences contamination was a major concern during the approach to Tempel 1 and bakes were scheduled at E-60 days, E-46 days, E-33 days, E-19 days, and E-3 days to deal with it.

The Camera Model

The camera geometric model is used to rotate a vector, \mathbf{t} , in inertial coordinates (such as the spacecraft-to-comet vector) into a vector, \mathbf{p} , in camera focal plane coordinates. This is accomplished in three steps. The first step is to rotate the vector \mathbf{t} from the International Celestial Reference System (ICRS) coordinates, into a frame whose z -axis is coincident with the camera optical axis, with $+z$ in the direction of the target; and whose x - and y - axes form a plane parallel to the nominal camera focal plane. The second step is to project these three-dimensional coordinates onto the camera focal plane. The third step is to scale the focal plane coordinates to camera sample (horizontal) and line (vertical) coordinates in pixels⁹.

First, we get the inertial to spacecraft body-fixed rotation matrix, \mathbf{T}_{i2bf} , from the spacecraft ACS system using information from the star-tracker. This was provided as right ascension α and declination δ of the camera boresight and twist φ of the scene about the boresight and as a quaternion in the NExT picture headers. In this case \mathbf{T}_{i2bf} is computed using equation (1):

$$\mathbf{T}_{i2bf} = \mathbf{R}_3(\varphi) \mathbf{R}_2(90-\delta) \mathbf{R}_3(\alpha). \quad (1)$$

When planning (rather than processing) pictures \mathbf{T}_{i2bf} is computed from the spacecraft trajectory with the body-fixed x -direction toward the target and the y -direction from the spacecraft to the sun. When Stardust was flying backwards towards the comet a rotation of 180° about the z -axis was applied to the nominal \mathbf{T}_{i2bf} . The rotation to camera coordinate system (M, N, L) is composed of the orientation of the M-N plane w.r.t. the X-Z plane, which depends on how the CCD is mounted in the camera, and a reflection of the image in the X-Z plane due to the scanning mirror. The camera orientation was determined from pictures taken during the prime mission. These factors are expressed in equation (2):

$$\mathbf{T}_1 = \mathbf{M}_1 \mathbf{R}_3(270^\circ) \mathbf{R}_2(90^\circ), \quad (2)$$

where

$$\mathbf{M}_1 = \begin{bmatrix} -1 & 0 & 0 \\ 0 & 1 & 0 \\ 0 & 0 & 1 \end{bmatrix}. \quad (3)$$

Equation (3) applies when the mirror angle, θ , is 0° . As the mirror rotates the boresight will sweep through the X-Z plane. Since the camera is fixed, the picture will appear to rotate around the boresight. This rotation is described by equation (4):

$$\mathbf{T}_2 = \mathbf{R}_3(\theta) \mathbf{R}_1(\theta), \quad (4)$$

where \mathbf{R}_1 is a positive rotation about +Y to align the boresight and \mathbf{R}_3 rotates around the boresight. There are also misalignments in elevation (χ), cross-elevation (Ω) and twist (Ψ) which vary with scanning mirror angle. These are taken care of by the rotations

$$\mathbf{T}_3 = \mathbf{R}_3(\Omega) \mathbf{R}_1(-\chi) \mathbf{R}_2(\Psi) . \quad (5)$$

The variations of Ω , χ , and Ψ with θ were calibrated for $\theta < 160^\circ$ during the prime mission. The complete transformation from inertial to camera frame coordinates, \mathbf{T}_{itv} , is

$$\mathbf{T}_{\text{itv}} = \mathbf{T}_3 \mathbf{T}_2 \mathbf{T}_1 \mathbf{T}_{\text{i2bf}} . \quad (6)$$

Finally,

$$\mathbf{P} = \mathbf{T}_{\text{itv}} \mathbf{t} . \quad (7)$$

The second step is accomplished by projecting \mathbf{P} into the focal plane using the ideal gnomonic projection,

$$\begin{pmatrix} x \\ y \end{pmatrix} = f \begin{pmatrix} P_1 / P_3 \\ P_2 / P_3 \end{pmatrix}, \quad (8)$$

where f is the camera focal length. Note that x , y and f have units of millimeters.

We account for distortions in the camera optics with

$$\begin{pmatrix} \Delta x \\ \Delta y \end{pmatrix} = \begin{pmatrix} -yr & xr^2 & -yr^3 & xr^4 & xy & x^2 \\ xr & yr^2 & xr^3 & yr^4 & y^2 & xy \end{pmatrix} \begin{pmatrix} a_1 \\ a_2 \\ a_3 \\ a_4 \\ a_5 \\ a_6 \end{pmatrix}, \quad (9)$$

where the a_i are a set of six distortion coefficients and $r^2 = x^2 + y^2$. The coefficient a_2 models the cubic radial distortion, and a_5 and a_6 represent the degree to which the detector is not orthogonal to the optic axis. The cubic radial distortion is the only non-zero distortion in our adopted model. The coefficients f and a_2 are noted in Table 2. The last step is to map the corrected x and y into the sample and line (CCD image) space with,

$$\begin{pmatrix} s \\ l \end{pmatrix} = \begin{pmatrix} s_0 \\ l_0 \end{pmatrix} + \begin{pmatrix} K_x & K_{xy} & K_{xxy} \\ K_{yx} & K_y & K_{yy} \end{pmatrix} \begin{pmatrix} x + \Delta x \\ y + \Delta y \\ (x + \Delta x)(y + \Delta y) \end{pmatrix}, \quad (10)$$

where (s_0, l_0) are the sample and line coordinates of the optical axis. This is taken to be the geometrical center of the detector. The matrix \mathbf{K} converts from millimeters to pixels. The center of the upper left pixel is (1, 1) and $(s_0, l_0) = (512.5, 512.5)$. During operations, K_x and K_y were set to 83.3333 and -83.3333 pixels/mm resp., and the remaining terms in the K-matrix set to zero.

The NavCam was calibrated October 17, 2000 and January 14, 2009. This is shown in Table 2.

Table 2. NavCam Geometric Calibration.

Parameter	Units	2000	2009
f	(mm)	201.209 ± 0.002	201.136 ± 0.005
a_2	(mm ⁻²)	$4.20 \pm 0.24 \text{ e-}5$	$5.24 \pm 0.07 \text{ e-}5$

The focal length had changed by less than 0.1%. The camera calibration was very stable. No geometric calibration was needed prior to approach.

The JPL TGP (Trajectory Geometry Program) has no provision for scanning mirrors. A picture-prediction script, first developed for the Deep Space 1 mission, and used on the Stardust prime mission, was used to apply the camera model to planning NExT pictures. During flight operations, TGP was supplied with the boresight pointing for each picture, corrected for the scanning mirror misalignments, from the script, and a \mathbf{K} -matrix that included the reflection from the scanning mirror. This allowed the processing of opnavs using flight-tested software.

THE ORIGINAL OPNAV SCHEDULE

We planned to take eight pictures at each imaging period, alternating between opnavs and science pictures. The science pictures would include just the comet window. The project decided on an imaging period every two hours. This provided sufficient time to rotate the spacecraft to and from the imaging attitude. The original opnav schedule consisted of two sets of opnavs per week from E-60 days to E-30 days, one set per day until E-14 days, and two sets per day from E-14 days to E-42 hours. This would be the last set of opnavs before the AutoNav system took over OpNav. The total of planned opnavs was 192. The opnavs would be exposed for 20 s and the science pictures for 10 s. Each OpNav set would provide a total exposure of 80 s when coadded. This schedule was very similar to the opnav schedule for the successful Wild 2 flyby. All the pictures, including science, except those from E-30 minutes to E+2 hours (which were handed by the AutoNav system) were planned by the OpNav team using the picture-prediction script. In case the bakes planned for Tempel 1 approach failed to decontaminate the NavCam, the design was to use 6th-8th magnitude stars to estimate the picture pointing.

IMAGING

For both science and OpNav, the spacecraft was moved from earth-point to the imaging attitudes by dead-band walks using the RCS thrusters. They maintained the spacecraft attitude to an accuracy of $\pm 0.25^\circ$ or 80 image pixels during the imaging periods. To minimize downlink time four 201x201 “windows” surrounding the comet and three reference stars were downlinked from each picture. The windows size was chosen to minimize the risk of the comet not being imaged in the window. The window locations were fixed in picture pixel coordinates and determined in advance based upon the latest spacecraft trajectory and comet ephemeris available when the pictures were planned. This is shown in figure 3a). The flight software had the capability to adjust the windows from on-board measurements of the pointing offset, from the stars in the field, but it was not reliable and so was not used.

Contamination did not build up as it had during the prime mission. This allowed us to estimate the pointing from 9th and 10th magnitude stars. A sufficient number of these (at least 2) was available within 150 pixels of the comet during the last two weeks of approach. The comet was sometimes as much as 50 pixels outside 201x201 pixel window. This was probably due to a combination of the expected pointing error and small errors (compared to the deadbanding) in the prediction of the windows. For these reasons, between E-7 days and E-42 hours a single 351x351 pixel comet window was used. The science team adopted the same window size; making 380 science pictures available as opnavs. These were added to the opnav schedule. See figure 3b).

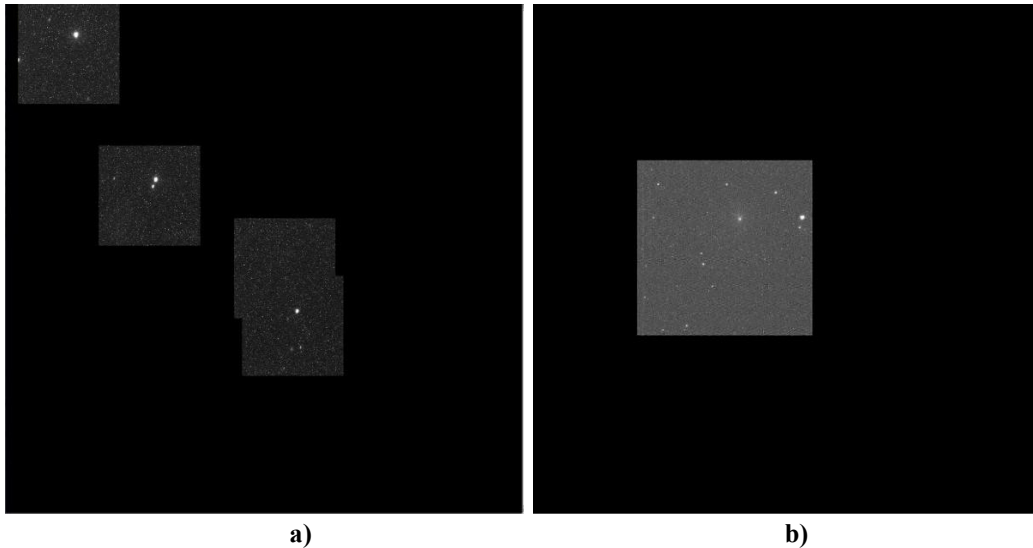


Figure 3a). An OpNav from December 17, 2010. It contains four 201x201 windows (see text). The remainder of the picture was not downlinked and so contains zeroes. The two windows on the left of the picture contain two bright astrometric reference stars. The two windows located right of center overlap. They contain a third reference star. The window nearest the center was placed at the predicted location of the comet. The comet was not visible in this exposure. **3b)** An opnav taken February 13, 2011. It contains one window. The comet is the bright, diffuse object above and to the right of the center of the window.

HOW THE MISSION DESIGN AFFECTED OPNAV PROCESSING

The largest factor driving the mission design was the small reserve of propellant. Downlink telemetry rates were determined primarily by the need to relax the pointing precision, whenever and for as long as possible, to minimize thruster firings and so minimize propellant use. The first

three weeks of science imaging were cut from the schedule. This had no effect on OpNav. This saved approximately 200 g of propellant; which was about 25% of the amount thought to be available in the tank. Until E-30 days Earth-pointing was maintained to $\pm 2^\circ$; allowing only the lowest downlink data rate of 504 bits/s. The telemetry stream included, in priority order, error messages, real time data, small force data, flight software data dumps, opnavs, and all other data. Small non-gravitational forces were continually exerted on the spacecraft by solar radiation and out-gassing from the spacecraft. Tracking these forces required frequent samples; which lead to a large amount of small force data compared to the opnavs. This meant that the point in the downlink window when the opnavs started to be received varied considerably. Downlinks taking more than 9-12 hours required multiple stations. Table 3 shows the minimum time taken to receive a set of eight pictures for various telemetry rates and data production rates.

Table 3. Opnav Downlink Times¹⁰.

Telemetry rate (Bits/s)	Production Rate (Bits/s)	Downlink time (Hours)		Telemetry rate (Bits/s)	Production Rate (Bits/s)	Downlink time (Hours)
15800	504	0.2		3950	504	1.0
12600	7900	0.4		1975	1975	10.6
12600	504	0.3		1975	504	2.2
7900	7900	0.8		1050	105	6.2
7900	504	0.5		1050	504	5.0
3950	3950	1.9		504	252	14.1
3950	1975	1.6		504	504	20.7
3950	1050	1.2				

At the start of the approach it took 21 hours from the beginning of a downlink to complete the receipt of an opnav set. The schedule accommodated this latency at this time. The NExT project really wanted to know when we first saw the comet. It quickly became clear that to do so required co-adding pictures in a set. This lead to a two-shift strategy; the OpNav team looked for the comet in the first two or three co-added pictures during the first shift and then looked at a co-addition of all the available pictures the next day.

At E-19 days we got 24-hour DSN coverage with, typically, one 70 m station each day. A picture set was on the ground within four hours of the start of the downlink over a 34 m station and within 90 minutes when a 70 m station was available. When two-hour imaging started at E-7 days Earth-point was maintained to $\pm 0.25^\circ$, to downlink the much greater volume of pictures in a timely manner. In fact, 0.25° deadbands were used continuously because frequent transitions from 2° to 0.25° deadband control used more propellant. During the critical period from E-80 hours to E-42 hours a combination of continuous 70 m coverage and MCD3 encoding ensured that picture sets were received within 90-mins of the start of the downlink.

HOW OPNAV FITS INTO FLIGHT OPERATIONS

OpNav is an essential part of the flight team on comet flyby missions. For NExT, the OpNav provided optical object (comet and stars) centers and picture pointing estimates to the OD team. It also provided astrometric measurements of the spacecraft-comet vector to the JPL solar system dynamics group (SSD). They used the opnavs, along with a radiometrically-determined spacecraft ephemeris and ground-based comet astrometry, to periodically update the comet ephemeris used by the navigation team. The ground-based astrometry was most sensitive to the time-of-flight of the spacecraft to the comet and so provided information that the opnavs did not. It also supplemented the comet declination measurements from the opnavs.

The OpNav team provided comet and star window updates, scanning mirror angle updates, and opnavs and science picture exposure durations to the spacecraft team at Lockheed-Martin Aerospace (LMA). The team also reviewed and verified spacecraft commanding, as it related to OpNav and science imagery, with the spacecraft team and science team prior to transmission to the DSN and uplink to the spacecraft.

Optical data from the spacecraft was received and recorded at one of several Deep Space Network (DSN) antennas around the world. It was transmitted to the JPL telemetry data system (TDS) where the optical data was stripped from the telemetry stream and sent to the Stardust data management and archive team. They assembled the opnav telemetry packets into pictures. These were available, typically, three times per day, after downlinks, for OpNav processing. The complete web of interfaces and processes is shown in Figure 4

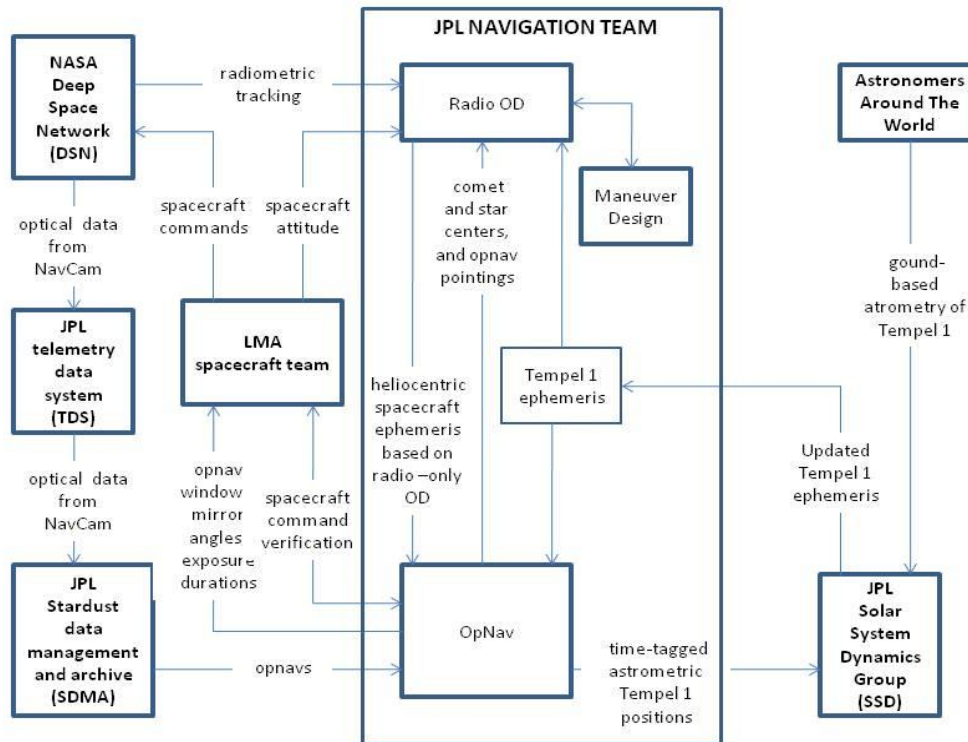


Figure 4. The Relationship of the OpNav Team to Flight Operations

CHALLENGES

There were a number of technical and logistical challenges during approach. Chief among these were a target comet that proved fainter than predicted, camera motion, scattered light, fixed-pattern noise, and data volume. The technical challenges are displayed in figure 5.

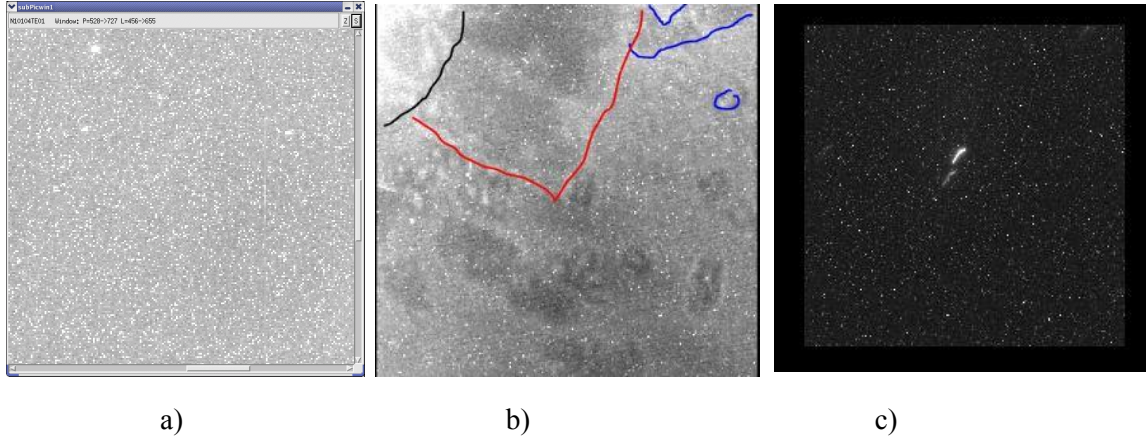


Figure 5. Technical challenges. a) Pattern-noise spikes. b) Background illuminated by stray light. A number of persistent patterns are visible from picture to picture. They are indicated by the black, red, and blue outlines. c) Smear images.

Comet Fainter Than Predicted

The expected comet signal was initially estimated to be more than 40 DN, in a 20 s exposure, at E-60 days¹¹ – making it easy to see. This was expected to double over the next 30 days. On 12/29/2010 this estimate was revised downward by the science team. In both estimates, images of the comet taken with the Deep Impact medium resolution imager (MRI) during the 2005 encounter are used to infer the coma signal in the central pixel of the camera PSF. It is assumed that only this pixel will be visible early on. This signal is then scaled to what would have been seen with the NavCam at the same time. It is then scaled to what would be seen during the NExT encounter.

The primary reason that the 3/29/2010 model overestimated the comet brightness is that it did not take into account that central pixel of the MRI PSF contained only 30% of this signal and that the NavCam central pixel would hold only 18% of the coma light. Another reason for overestimating the comet brightness is that the comet model used in the 3/29/2010 estimate does not include the opposition effect. This was accounted for in the 12/29/2010 model by reducing the geometric albedo of the nucleus by about 25%. A fixed coma/nucleus signal ratio of three was assumed in the 3/29/2010 estimate. This overestimated the nucleus signal at E-60 days when the phase angle was small¹². It became unlikely that we would see the comet before E-30 days. Figure 6a) compares the original brightness estimate with the one adopted on 12/29/2010. Figure 6b) shows that the revised estimate agreed quite well with the actual comet brightness.

Tempel 1 was first detected in the E-26 days (1/19/2011) opnavs, more than a month later than originally expected and less than a month before encounter. A 160-second co-add of eight pictures showed 4-6 pixels at the brightness peak, totaling 20-24 DN above the background (with 6 DN in the central pixel). We got about the expected count rate from the comet. Fortunately, these pictures suffered little smear so that we detected the comet at the earliest opportunity.

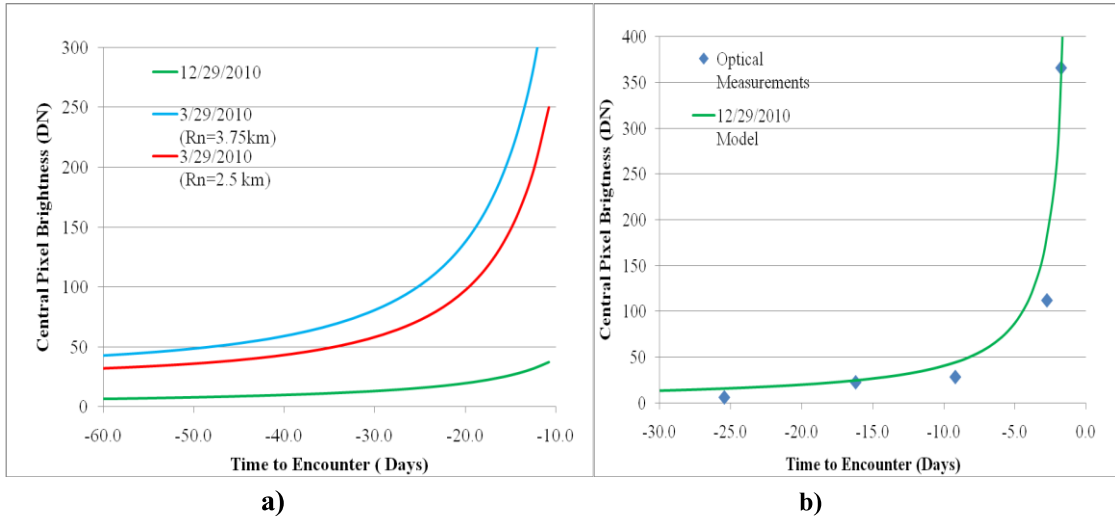


Figure 6. Central pixel brightness of 9P/Tempel 1 in an un-smearred 20 s exposure. a) Comet brightness models. Two cases of the 3/29/2010 model are shown that bound the size of the nucleus. b) The revised model vs. central brightnesses from actual comet images.

Camera Motion

Camera motion caused star images to be smeared up to 25 pixels. The amount of motion was dependent on the instantaneous attitude rates, and these depended on the angular momentum of the spacecraft, which in turn depended partly on the moment provided by the RCS thruster pulses and partly on the torque from solar pressure. If the latter was negligible, then the spacecraft would bounce back and forth between the deadband limits, with a thruster firing at each limit. If the external torques were appreciable and acted in the same direction during the imaging period, then the attitude would follow a sequence of parabolic arcs, with the thrusters firing on only one side of the deadband. Typically the thrusters fired two or three times during the imaging periods. Their pulses were only 15 ms in duration and so can be considered instantaneous in comparison to the imaging periods. Image smear was usually similar for consecutive pictures. The amounts of smear and the exposure durations provide a measure of the rate of motion of the spacecraft between pulses. The total motion can be estimated between thruster firings. In the few imaging sequences investigated, the total distance moved between thruster firings was considerably greater than the 78 pixels expected for single-sided deadbanding with a range of 0.25° . It is likely that double-sided deadbanding was taking place.

During the period 25-29 January, prior to TCM-32, image smear was consistently large, ranging from 2-3 pixels to 24-25 pixels. Only 7 of 32 pictures had less than 4 pixels of smear. This made 1/3 of them useless for OpNav. OpNavs were critical to the design of TCM-32. To minimize the risk of postponing this maneuver further and the concomitant risk of making an error in the maneuver design, and so putting the flyby in jeopardy, the nav. team decided to reduce the durations of the opnavs taken from E-13 days (2/2/2011) to E-10 days (2/5/2011) to 10 s to reduce smear.

Only 2 of the 32 pictures taken from 2/2/ to 2/5 were smeared more than 4 pixels. This improvement was much greater than that expected from halving the exposures. The signal rates were generally a little smaller than predicted but, ultimately, sufficient.

New software was developed to characterize the stellar point-spreads in each picture and, with deconvolution techniques, sharpen them and the comet images. We had some success in sharpening the stars but could not bring up the comet to be visible in individual, background-subtracted pictures taken before E-7 days. After this time, deconvolution was not needed.

Scattered Light

Light scattered into the camera from undetermined spacecraft structures produced an increasing background that varied in a complex way over time-scales of several minutes. By E-36 days (1/10/2011) the brightest of the stars intended for pointing estimation were saturated; reducing the usefulness of the star windows. The background varied spatially due to the illumination of residual contamination on the optics near the CCD chip. At E-25 days (1/18/2011) we responded to the worsening background by adjusting the flight profile to fix the scan mirror angle for imaging at 160°. This moved the illumination off the structures which scattered light, and reduced the background level to that expected from the sum of the bias level and dark current accumulation. The background had increased slowly by 500 DN by E-13 days (2/22/2011). In the next 24 hours it increased by another 300 DN. This was remedied, at E-7 days, by rotating the spacecraft 180° about the z-axis so that mirror angles of approximately 20° could be used for imaging. Experience from the prime mission had shown that this configuration would not suffer from scattered light¹³ and, indeed, the background returned to near the value expected from electronic offsets.

Fixed-Pattern Noise

The NavCam suffers from a fixed-pattern of radiation-damaged high pixels which reduces its sensitivity. Power-cycling the camera greatly reduced the density and amplitude of this pattern-noise. However, each power-cycle ran the risk of a failure of the power supply for the camera electronics. (A similar power supply, this one for the camera filter wheel, had failed in 2001.) Consequently, the project decided not to power-cycle it more often than absolutely necessary. OpNav was allotted twelve power-cycles which were used to “protect” the pictures supporting the Autonav initialization and the pictures immediately prior to the maneuver data-cutoffs. Initially, pattern-noise was reduced during processing by zeroing pixels above a threshold selected for each picture. This also required new software.

Background Subtraction

Pictures were preprocessed with MatLab™ scripts developed during approach. The scattered-light background was estimated as the temporal median of the available raw pictures in a set. Nominally, they were all of the same part of the sky. However, the expected random pointing offsets ensured that each picture carried the scene on different pixels. Thus, the median rejected the objects and kept the background and fixed-pattern noise spikes. The background was then subtracted from the pictures, leaving a very small residual background with much less contrast in each. This completely removed the pattern noise spikes. The cleaned pictures were co-registered using pointings estimated from the stars in them. A constant was added to each picture to ensure that there were no negative DN values in the final pictures as these confused the center-finding

routines. Astrometry was then performed on the pictures using the JPL optical centerfinding and astrometry software.

Data Volume

The main logistical challenge was to keep up with the flow of pictures to process, particularly between E-7 days and E-100 hours. A backlog of pictures occurred and some were lost, when two-hour imaging started. This was resolved by turning off the return of ranging data from the spacecraft during some of the 34 m tracks between E-7 days and E-3 days to provide more time for opnavs and reduce the backlog. The one 70 m track per day was then sufficient to “catch up”. During this period opnav bits were being dropped, leading to some unusable pictures, because the spacecraft was taking too long to return to Earth-point after imaging. This was remedied by slewing the spacecraft at a higher rate to be on Earth-point at the start of the tracking pass.

COMET MEASUREMENTS

Sets of eight opnavs were taken nearly daily from E-25 days to E-9 days. We provided optical comet positions, based on co-addition of the available frames in each set, throughout this period. The measurements were time-tagged at the average of the individual picture times.

TCM-31 was postponed 24 days to E-16 days (1/31/2011) while we accumulated sufficient opnavs to determine the extent of the expected difference between the ground-based comet ephemeris and the actual comet position. The purpose of TCM-31 was to make a gross correction to the trajectory to meet the comet. From E-14 days (2/1/2011), a day earlier than planned, we scheduled and processed two sets of opnavs per day to provide enough pictures to offset losses due to smear and ensure sufficient opnav information to design TCM-32. This maneuver was delayed from E-11 days (2/4/2011) to E-8 days (2/7/2011) because of the delay of TCM-31. Between E-16 days and E-8 days we scheduled and processed ten sets of opnavs. The TCM schedule resulting from when the comet was first detected is depicted in Figure 7.

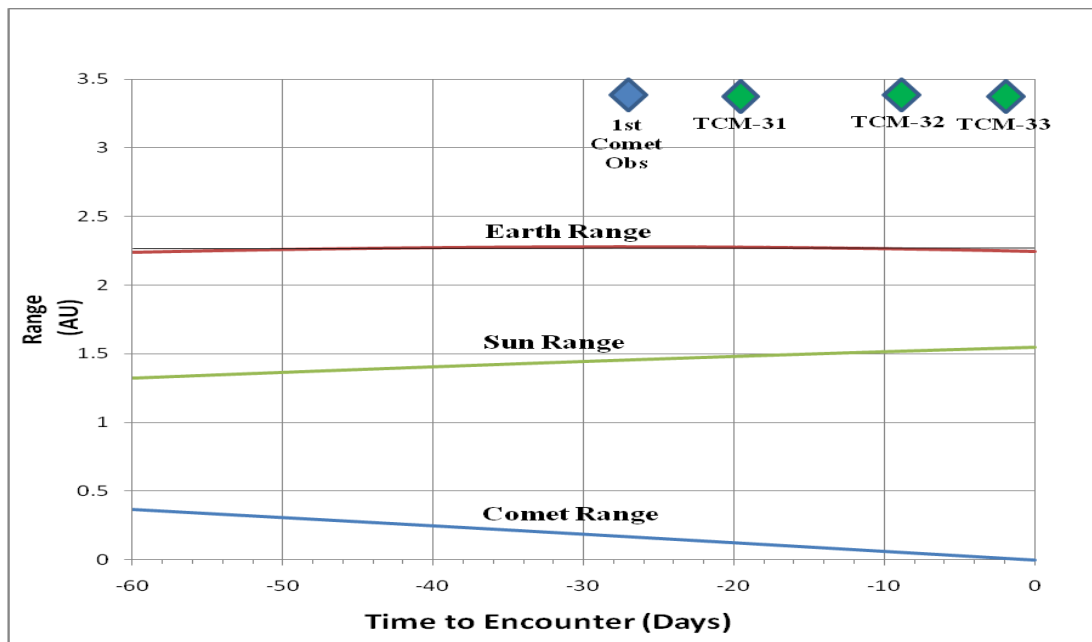


Figure 7. Approach Overview.

OpNav contributed increasingly to the three comet targeting maneuvers; TCM-31, TCM-32 and TCM-33. The weakness of the comet signal and the various noise sources in the pictures limited the precision of the optical centers. The OpNav team offered a very tentative weight (one-sigma) of 1-1.5 pixels on first measurement (1/19/2011). This was not sufficient to support a credible comet ephemeris update. It was sufficient at TCM-31 to constrain deviations from the prediction to approximately 2500 km. Knowledge of the spacecraft to comet vector, from opnavs, improved as the comet range decreased. From 1/19 to 1/29, when the first astrometric comet position was delivered to the SSD group, the weight on the optical measurements steadily decreased to 1.0 pixel. The optical weights decreased to 0.75 pixel by 2/1/2011. With these measurements, OpNav confirmed the need for a planned maneuver to correct the B-plane by 350 km at TCM-32. We offered weights of 0.5 pixel between 2/7 and 2/12. These dropped to 0.25 pixel through E-42 hours. Comet residuals prior to the planned, twelve-hour, camera bake at E-99 hours (2/11/2011 01:30 UT) contained the suggestion of a sinusoidal variation. The pattern appeared to continue after the bake from E-82 hours to E-76 hours, the data-cutoff for TCM-33. This is shown by the red curve in figure 8. The concern was that we were seeing the offset between the center of brightness and the center of mass of the nucleus as it rotated. A trajectory correction for this non-gravitational offset would have been needed.

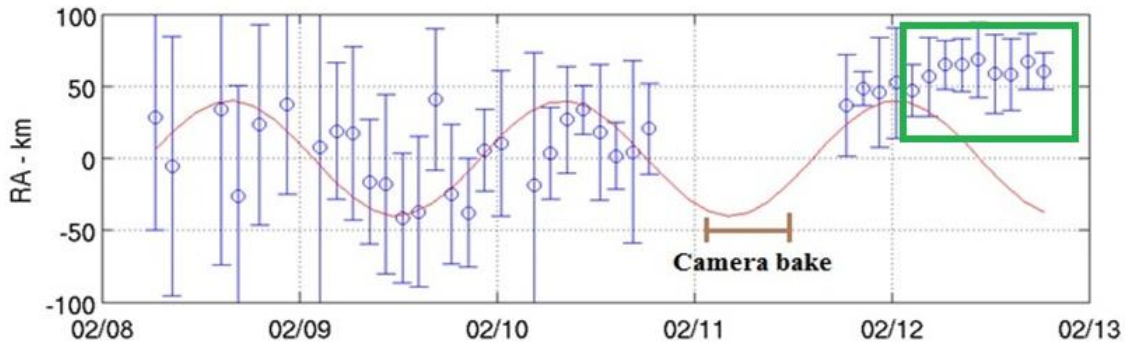


Figure 8. Comet position residuals. The residuals after the TCM-33 data cut-off, at E-76 hours, are in the green rectangle.

The navigation and science teams decided that it was unlikely that we were seeing a center-of-mass/center-of-brightness offset. The evidence was at best only suggestive. The decision was made to base TCM-33 upon the supposition that the opnavs after the camera bake were indicating the continued decrease of the bias introduced by the difference between the centers of brightness of the coma and the nucleus. In this case a different correction, perhaps quite small, would be required to hit the B-plane target. The residuals continued to increase through E-42 hours, instead of decreasing as would have been expected from continued sinusoidal behavior. The opnavs from E-76 hours to E-42 hours confirmed that we were seeing the center of brightness shifting away from the coma to the nucleus. They confirmed that the right choice of maneuver had been made at E-42 hours.

By the start of the approach phase, the navigation and science teams had determined to fly by the comet at 180-230 km. This demanded navigating the spacecraft to the B-plane target with a precision of approx 10 km, one-sigma. At the TCM-33 data cut-off the spacecraft to comet range was 1.5 million km. The comet nucleus is about 3 km in size. Better than 0.1 pixel precision was required of the comet center-finding at this time. OpNav was able to provide centers with 0.25 pixel sigmas on single measurements. We had eight instead of the planned four pictures in the set

at the TCM-33 data-cutoff. This set was statistically as precise, with 0.25 pixel sigmas on each picture, as the originally planned set with 0.1 pixel sigmas on each picture.

Opnavs and ground-based observations of the comet from several observatories allowed the continual improvement of its ephemeris by the SSD group. The initial estimate of the comet location at the flyby, from ephemeris k053_25, see figure 9a), was based entirely on ground-based astrometry. (It used data collected in a thirteen-year observing campaign.¹⁴) Between 2/3/2011 and 2/10/2011, comet position estimates, from ephemerides 98, 117 and 121, consistently showed that the comet had moved in the B-plane approximately 450 km from the k053_25 estimate. The errors decreased from approximately ± 700 km (1-sigma) to approximately ± 50 km. Solution 145 indicated the same 50-70 km walk seen in the residuals on 2/13/2011. The subsequent ephemeris 150, from the SSD group, which included opnavs taken at E-42 hours, indicated that the walk had grown to 100 km. It also indicated that the comet position errors were down to the required ± 10 km. This is shown in Figure 9b).

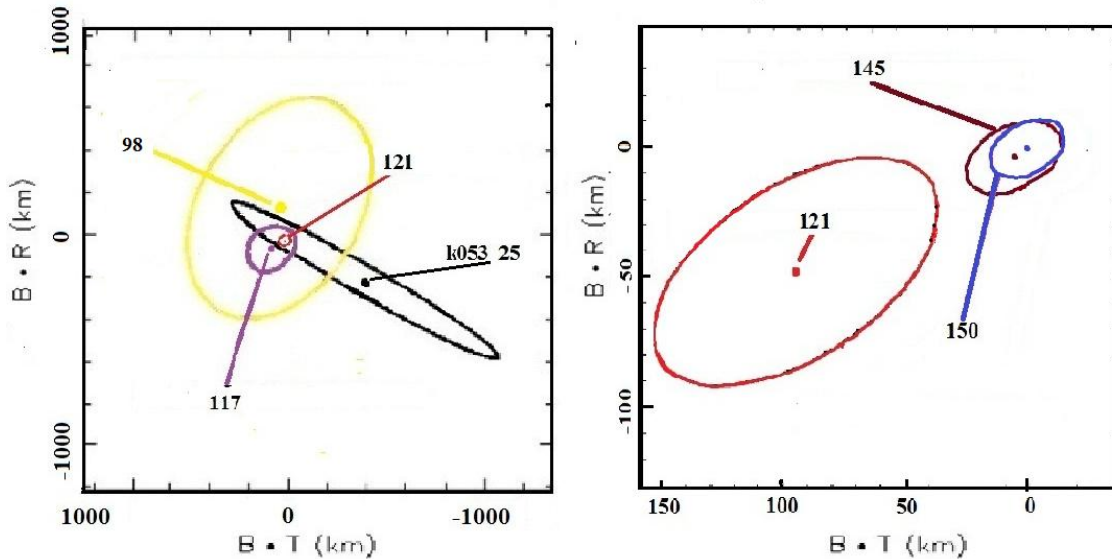


Figure 9. Evolution of delivered Temple 1 ephemeris B-plane and 1-sigma uncertainties therein, referred to solution 150. a) 12/17/2010 to 2/10/2011 and b) 2/10/2011 to 2/13/2011.

Ephemerides K053_25, 98, and 121 were used in the designs of TCM-31, TCM-32, and TCM-33 respectively. Solution 145 and the comet centers from the opnavs at E-42 hours were used by the OD team to estimate the a-priori ephemeris supplied to the Autonav filter.

STAFFING

The OpNav team started with one person in April 2010. This was sufficient to set up the picture processing software and carry out the initial picture planning. The team was increased to three people a month before approach. This provided time to train them on the software. We added another opnav analyst in mid-January 2011 to help with the larger than expected workload due to the need to carry the previously discussed picture pre-processing. We added one more team member in early February 2011 to help with the review and validation of command products. There were two other optical navigators available as advisors; one of whom was the OpNav lead during the prime mission.

PICTURE STATISTICS

The original OpNav schedule included 192 pictures. The scheduling of the extra pictures between TCM-31 and TCM-32 and the addition of the two-hour science imaging to the opnav schedule increased the number of planned opnavs to 638. Eighteen of these were not down-linked. We used 552. Eighty-six were unusable because they were smeared more than ten pixels, or the comet was not in the window, or they could not be processed because of readout errors, or the pictures were missing lines through the comet.

LESSONS LEARNED

We recommend that future missions include reaction wheels for attitude control. Images would not have been smeared and a gain of 2-5 in comet signal-to-noise, over that from images smeared up to 25 pixels, would have obviated the need to schedule extra pictures between TCM-31 and TCM-32. There would have been less contention with small forces telemetry during the down-links between E-7 days and E-3 days.

The calculations of the expected comet brightness should have been reviewed by the navigation and science teams together before TCMs 31, 32 and 33 were scheduled. The error in the original estimate would have been found, and a better idea of when the comet would first be detected would have resulted. This would have avoided the several reschedules of the TCMs and the risk involved in such late changes to the flight plan.

CONCLUDING REMARKS

This was a very challenging mission for the OpNav team due primarily to the limitations of the flight system and the defects in the NavCam. The OpNav team, the navigation and spacecraft teams, and the Stardust-NExT project met every challenge efficiently. The care, dedication, and sheer hard work of the navigation and spacecraft teams made Stardust-NExT an outstandingly successful mission.

We called upon all the expertise available in the JPL navigation section to ensure the success of the mission. Success was also assured by the flexibility of the OpNav team, in building new software to pre-process the pictures and in processing them at all hours of the day and night. The project was also very flexible in authorizing extra staff to analyze the larger-than -planned volume of opnavs and verify command products on an almost continuous basis between E-21 days and E-7 days. The spacecraft team was also very flexible in re-designing and testing, at times at very short notice, command sequences in response to the issues discussed in this paper. This effort demanded and received the excellent cooperation of the spacecraft and OpNav teams.

It is remarkable that we were able to go from the opnav in figure 10a) to the closest approach science picture in figure 10b)

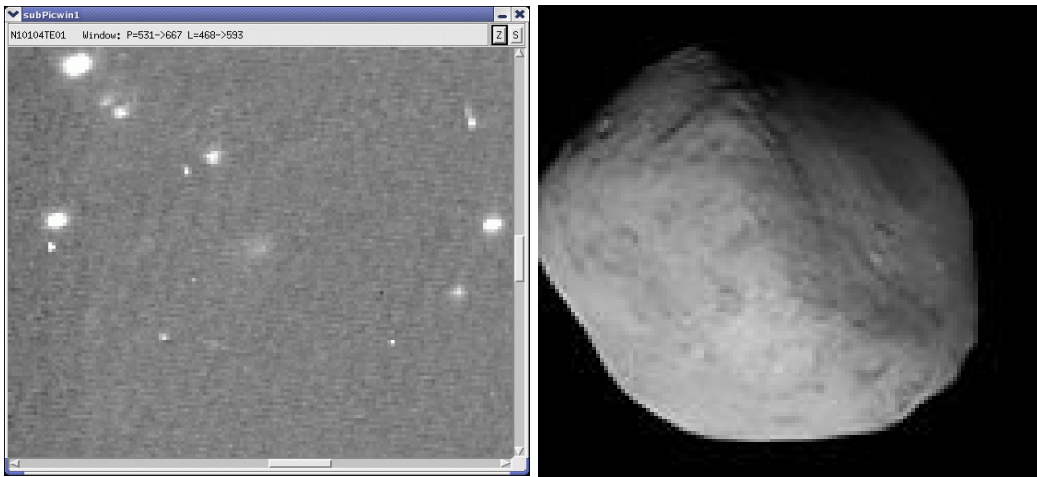


Figure 10. Tempel 1 from first observation to closest approach. a) The first observation of Tempel 1 on 1/19/2011. The comet is the fuzzy blob near the center of the picture. The signal-to-noise in this coadd of eight pictures is approximately six. b) The science picture of the nucleus at closest approach (178 km).

ACKNOWLEDGMENTS

The research described in this paper was carried out by the Jet Propulsion Laboratory, California Institute of Technology, under a contract with the National Aeronautics and Space Administration. Thanks to Allan Chevront and Kevin Gilliland of Lockheed Martin Aerospace for their very helpful answers to many questions during the mission and during the writing of this paper.

Copyright 2011 California Institute of Technology. Government sponsorship acknowledged.

REFERENCES

- ¹ Thomas C. Duxbury, Ray L. Newburn, Charles H. Acton, Eric Carranza, Timothy P. McElrath, Robert E. Ryan, Stephen P. Synnott, and T. Han You, "Asteroid 5535 Annefrank size, shape, and orientation: Stardust first results." *Journal of Geophysical Research*. Vol. 109, 2004.
- ² Ron Baalke and Aimee L. Meyer (Stardust education and public outreach team), "STARDUST-NExT Exploration of Comet Tempel 1." http://stardustnext.jpl.nasa.gov/mission/sci_objectives.html.
- ³ J. Raymond B. Frauenholz, Ramachandra S. Bhat, Steven R. Chesley, Nickolaos Mastrodemos, William M. Owen Jr., and Mark S. Ryne, "Deep Impact Navigation System Performance." *Journal of Spacecraft and Rockets*. Vol. 45, No. 1, 2008, pp. 39–56.
- ⁴ Joseph Veverka, Benton Clark, Kenneth Klaasen, Don Brownlee, Thomas Duxbury, Karen Meech, Jessica Sunshine, Peter Schultz, H. Melosh, Robert Farquhar, Johan Silen, Teemu Mäkinen, Michael A'Hearn, Jochen Kissel, Steven Chesley, Michael Belton, Thanasis Economou, James Richardson, Olivier Groussin, Peter Thomas, "Stardust-NExT A Mission to Complete the Exploration of Comet Tempel 1 with Stardust." *Proposal submitted to the National Aeronautics And Space Administration*. NASA proposal number 06-DISC06-0005, 13 March 2007.
- ⁵ William M. Owen Jr., N. Mastrodemos, B. P. Rush, T.-C M. Wang, S. D. Gillam, S. Bhaskaran, "Optical Navigation For Deep Impact." *Proceedings of the 16th AAS/IAA Space Flight Mechanics Conference*, AAS-06176.
- ⁶ Shyam Bhaskaran, Joseph E. Riedel, and Stephen P. Synnott "Autonomous Nucleus Tracking for Comet/Asteroid Encounters: The Stardust Example." *Aerospace Conference, 1998, Proceedings*. IEEE, Vol. 2, 1998, pp 353-365.

⁷ George Frascetti, Mark Schwochert, and Tom Radey, "Stardust Navigation Camera." <http://pdssbn.astro.umd.edu/holdings/sdu-a-navcam-2-edr-annefrank-v2.0/document/scdesc/camera.htm>.

⁸ Raymond L. Newburn, "Pictures of the Stardust Navigation Camera." http://pdssbn.astro.umd.edu/holdings/-stardust-c_e_l-nc-2-edr-v1.0/document/images/nc_cad3.gif.

⁹ B. Semenov, "Navigation Camera State History." <http://pds-smallbodies.astro.umd.edu/holdings/-sdu-c-navcam-5-wild2-shape-model-v2.0/catalog/navcam.cat>.

¹⁰ Allan Cheuvront, *Private communication*. January 8, 2011

¹¹ Olivier Groussin, Mike Belton, Mike A'Hearn, "Early detection of the nucleus of comet 9P/Tempel 1 by the Stardust-NExT mission." *Report to the Stardust-NExT Project*. March 29 2010.

¹² Kenneth Klaasen, *Private communication*. December 29, 2011.

¹³ Shyam Bhaskaran, Nick Mastrodemos, Joseph E. Riedel, Stephen P. Synnott, "Optical Navigation for the Stardust Wild 2 Encounter." *Proceedings of the 18th International Symposium on Space Flight Dynamics (ESA SP-548)*. 11-15 October 2004, Munich, Germany., p.455.

¹⁴ K.J. Meech, J. Pittichová, B. Yang, A. Zenn, M.J.S. Belton, M.F. A'Hearn, S. Bagnulo, J. Baif, L. Barrera, J.M. Bauer, J. Bedient, B.C. Bhatt, H. Boehnhardt, N. Brosch, M. Buie, I. P. Candia, W.-P. Chen, S. Chesley, P. Chiang, Y.-J. Choi, A. Cochran, S. Duddy, T.L. Farnham, Y. Fernández, P. Gutiérrez, O.R. Hainaut, D. Hampton, K. Herrmann, H. Hsieh, M.A. Kadooka, H. Kaluna, J. Keane, M.-J. Kim, J. Kleyna, K. Krisciunas, T.R. Lauer, L. Lara, J. Licandro, S.C. Lowry, L.A. McFadden, N. Moskovitz, B.E.A. Mueller, D. Polishook, N.S. Raja, T. Riesen, D.K. Sahu, N.H. Samarasinha, G. Sarid, T. Sekiguchi, S. Sonnett, N. Suntzeff, B. Taylor, G.P. Tozzi, R. Vasundhara, J.-B. Vincent, L. Wasserman, B. Webster-Schultz, and H. Zhao "Deep Impact, Stardust-NExT and the behavior of Comet 9P/Tempel 1 from 1997 to 2010." *Icarus*. Vol 213, Issue 1, May 2011, pp 323-344.